

Main-Chain Nonlinear Optical Polymers with Enhanced Orientational Stability

Martin Döbler, Christoph Weder, Oscar Ahumada, Peter Neuenschwander, and Ulrich W. Suter*

Institute of Polymers, Department of Materials, Swiss Federal Institute of Technology (ETH), CH-8092 Zürich, Switzerland

Stéphane Follonier, Christian Bosshard, and Peter Günter

Nonlinear Optics Laboratory, Institute of Quantum Electronics, Swiss Federal Institute of Technology (ETH), CH-8093 Zürich, Switzerland

Received July 6, 1998; Revised Manuscript Received August 31, 1998

ABSTRACT: Polyamides based on 2',5'-diamino-4-(dimethylamino)-4'-nitrostilbene (DDANS) and aliphatic diacids, and polyamideesters based on DDANS, 4-(bis(2-hydroxyethyl)amino)-benzaldehyde-1,1-diphenylhydrazine (BBDH), and adipic acid represent a promising class of polymers for nonlinear optic (NLO) and photorefractive applications, where the nonlinear optical units are fixed in the polymer backbone with their dipole moments oriented transversely to the main chain. The orientational relaxation behavior of a series of random copolymers and block copolymers was investigated at different temperatures below the glass transition by the decay of the nonlinear optical susceptibilities of corona-poled thin films. The time dependence of the decay was found to be well represented by the Kohlrausch–Williams–Watts stretched-exponential function. The temperature dependence of the decay could be correlated with the glass transition temperature T_g using a normalized relaxation law with $(T_g - T)/T$ as the relevant scaling parameter. The investigation of the thermal stability of the NLO-phore received special attention in this study. The main-chain polymers investigated exhibit an enhanced orientational stability when compared to side-chain or guest–host systems.

I. Introduction

In recent years there has been a significant interest in nonlinear optical (NLO), electrooptical (EO), and photorefractive (PR) polymers because of their potential use in efficient, ultrafast, and low-voltage integrated electrooptical devices as well as for optical storage applications.¹ The frequently cited advantages of poled polymers are large nonlinear susceptibilities and EO coefficients, fast response times, and easy processability. However, additional requirements such as long-term stability of the NLO or EO effect, high physical and chemical stability, and low optical propagation losses must be satisfied, before polymeric materials can demonstrate their potential as actual device materials.¹

We have developed a new approach to the design of NLO polymers with large and stable second-order nonlinear susceptibilities.^{2–10} In these polymers, the NLO-phores are part of the polymer backbone, with their dipole moments oriented transversely to the polymer main chain, a consequence of the assumption that in this arrangement the NLO-phores can easily be oriented (above the glass transition temperature) by an external electrical field but exhibit an improved orientational stability when compared to guest–host or side-chain NLO polymers. Within the framework of this new concept, we have reported the preparation of a series of semiflexible polyamides based on the bifunctional NLO-phore 2',5'-diamino-4-(dimethylamino)-4'-nitrostilbene (DDANS) and different linear aliphatic diacid dichlorides (Figure 1).² Large second-order nonlinear optical coefficients (d_{33}) of up to 40 pm/V at a fundamental wavelength of 1542 nm have been determined, using a standard Maker fringe technique.² To demonstrate the usefulness of these new NLO polyamides in actual

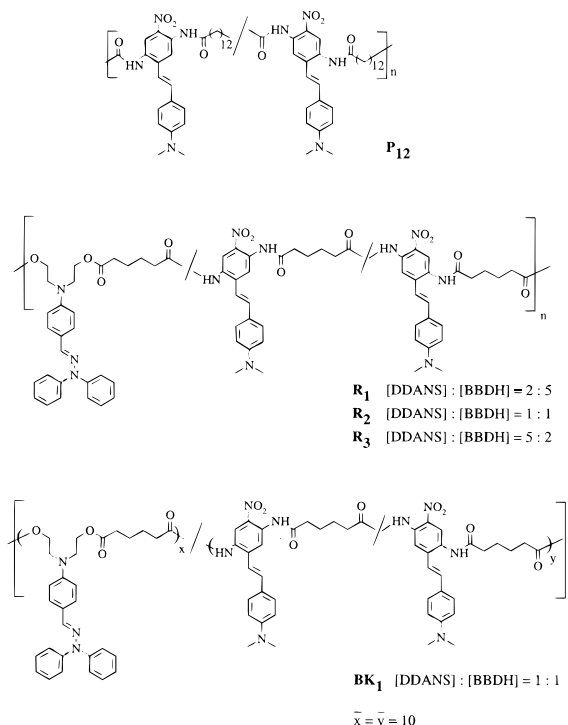


Figure 1. NLO polyamides and polyamide esters under investigation.

devices, the electrooptical properties of planar waveguides were investigated using attenuated total reflectance (ATR) spectroscopy, revealing electrooptical coefficients (r_{33}) of up to 12 pm/V (785 nm).⁷ Recently, we reported the photoconductive and photorefractive properties of these materials⁹ and also the preparation of a new class

Table 1. Physical Properties of the Main-Chain NLO Polymers

polymer	type of polymer system	T_g (°C)	η_{inh} (dL/g)	DDANS/BBDH mol/mol
P₁₂	polyamide	125	0.39	
R₁	random copolymer	80	0.40	28:72
R₂	random copolymer	111	0.40	56:44
R₃	random copolymer	131	0.41	72:28
BK₁	block copolymer (theoretical block-length 10)	80 and 160	0.21	55:45

of polymers for photorefractive applications based on DDANS, 4-(bis(2-hydroxyethyl)amino)benzaldehyde-1,1-diphenylhydrazine (BBDH), and aliphatic diacid dichlorides (Figure 1).¹⁰

Orientational relaxation experiments have revealed a remarkable orientational stability for the DDANS-based polyamides.³ However, when aged at elevated temperatures and *under air*, even at temperatures significantly lower than the decomposition temperatures determined by differential scanning calorimetry (DSC) and thermogravimetric analysis (TGA), a significant decomposition of the NLO-phore could be detected. This thermal decomposition process was found to be a limiting factor for the long-term behavior of the nonlinear optical susceptibility of the polyamides investigated.³ In the present paper, we have revisited the relaxation behavior of these materials, carefully investigating the thermal decomposition of the NLO-phore, and minimizing this effect by aging the samples under vacuum. In addition, the orientational stability of the high- T_g polyamideesters specially designed for photorefractive applications was explored.

II. Results and Discussion

Samples. The polymers investigated here include one representative example of the series of NLO polyamides based on DDANS and linear aliphatic diacids investigated before (**P₁₂**), and a series of NLO polyamide esters consisting of random copolymers (**R₁**, **R₂**, **R₃**) and a block copolymer (**BK₁**) based on DDANS, BBDH, and adipic acid. The random copolymers differ in the molar ratio of DDANS/BBDH, which was adjusted to about 1:2.5 (**R₁**), 1:1 (**R₂**), and 2.5:1 (**R₃**). A DDANS/BBDH molar ratio of about 1:1 was chosen for the block copolymer **BK₁**, which has a theoretical average block length of 10. Synthesis and characterization of these polymers are described elsewhere, including detailed linear and nonlinear optical measurements.^{2,3,9,10} The chemical structures of all polymers are shown in Figure 1, their physical properties relevant to this work are summarized in Table 1. A detailed description of the sample preparation is given in the Experimental Section.

Thermal Stability. As discussed in an earlier contribution,³ and also by other researchers,^{11–13} limitations for the long-term performance of poled NLO polymers can arise from the thermal instability of the NLO-phore. The spectrophotometric investigation of the NLO-phore's charge-transfer (CT) band is an excellent tool to investigate the long-term thermal stability of the NLO-phores in polymers.³ Here we employ this technique to investigate the thermal stability of the DDANS-based polymers in a wide temperature range *in a vacuum* and also *in air*. Thermal stability experiments are reported here for the polyamide **P₁₂** and the polyamideester **R₂** as representative examples for their respective series. A representative set of experiments is shown in Figure 2 for copolymer **R₂**.

As a measure for the NLO-phore concentration, the absorption coefficient α of the CT-band of the DDANS moiety at 474 nm was monitored as a function of time for samples that have been stored under either vacuum or air and at different temperatures (for the sake of readability of the graphs, only three to four spectra taken at different times of the aging process are shown for each temperature, however, at least five to seven spectra were used for the evaluation of decomposition times, see below). While at temperatures above 110 °C, a considerable decay of the NLO-phore's CT absorption could be detected for any of the polymers, the absorption band of the BBDH moiety, which can be observed at 364 nm, remains relatively constant. However, a slight increase of absorption, which is assumed to arise from products formed by the thermal decomposition of NLO-phores, is observed at this wavelength. This behavior is consistent with the assumption that the hydrazone moiety is more stable than the NLO-phore, and hence, no fundamental difference in thermal stability between the pure polyamides and the copolymers is likely.

The decrease of the NLO-phore concentration (as determined above) was found to follow a single-exponential decay for aging in a vacuum as well as in air, consistent with first-order decomposition kinetics (cf. Figure 3). Fitting this decrease, using the CT-band's absorption $A(t)$ as a function of time t allowed for the determination of the characteristic decomposition times δ

$$A(t) = A(0) e^{-t/\delta} \quad (1)$$

The decomposition times determined for polymers **P₁₂** and **R₂** under various conditions are shown in Figure 4. This graph shows clearly that polyamide **P₁₂** and polyamideester **R₂** exhibit similar thermal stabilities. However, a major influence of the aging conditions is evident. Samples stored in a vacuum exhibit a significantly improved thermal stability when compared to samples stored in air, especially at lower temperatures. To quantify this behavior, the Arrhenius activation energies E_A for the thermal decomposition were determined by fitting to eq 2. For the decomposition in a vacuum, E_A was found to be ca. 1600 kJ/mol, compared to a value of 1000 kJ/mol for decomposition in air.

$$\delta(T) \propto e^{-E_A/RT} \quad (2)$$

Orientational Stability. The orientational relaxation of the NLO-phores was investigated at different temperatures below the glass transition by the decay of the nonlinear optical susceptibilities d_{33} of corona-poled thin films using a standard Maker fringe technique at a fundamental wavelength of 1338 nm.^{2,10} All aging experiments were performed at temperatures well below the glass transition temperature, because annealing close to or above the glass transition temperature might result in significant structural changes. A full description of the experimental setup was given before, together with a detailed discussion of the linear and nonlinear optical properties of all polymers discussed here. An overview of the nonlinear optical properties of all polymers is given in Table 2.^{2,10,14}

For all relaxation experiments at elevated temperatures, samples were stored in a vacuum, while experiments at 25 °C were carried out with storage under ambient conditions. The NLO susceptibility $d_{33}(t)$ was monitored in intervals over a time of up to 9 months.

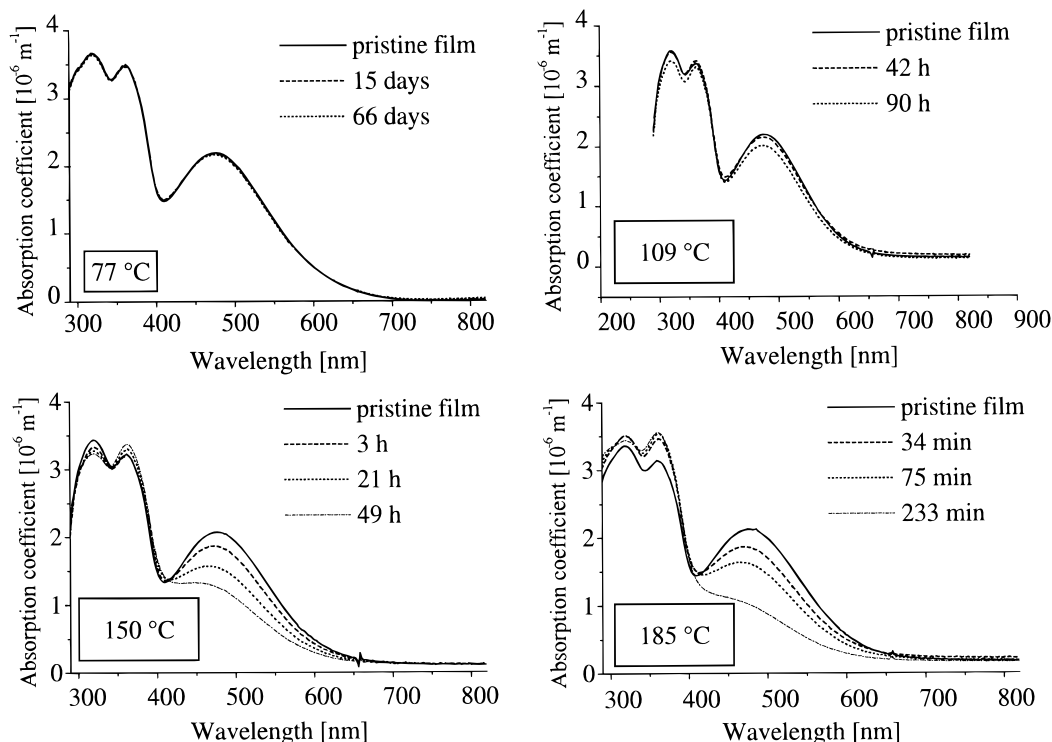


Figure 2. Thermal stability of thin films of polymer **R**₂. The absorption coefficients α were measured after different intervals of thermal aging at 77, 110, 150, and 185 °C.

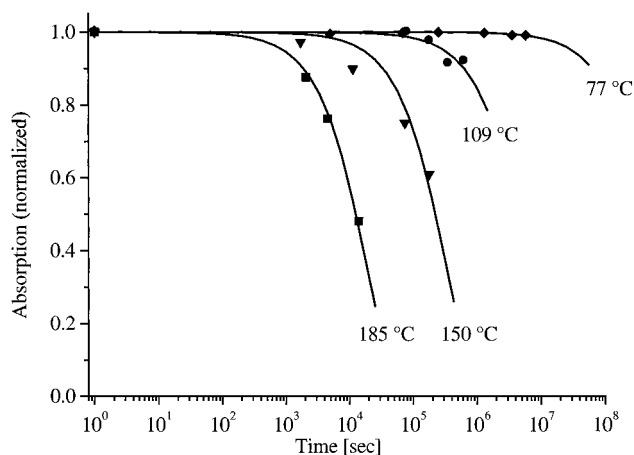


Figure 3. Decay of the normalized absorption of the NLO-phore's CT band at 474 nm in a thin film of polymer **R**₂, aged at different temperatures in a vacuum. Symbols refer to measured data, while the solid lines correspond to single-exponential fits according to eq 1.

Figure 5 shows the measured decay of d_{33} for polymers **P**₁₂, **R**₁, **R**₂, **R**₃, and **BK**₁ as a function of time and temperature in semilogarithmic representations. For the relaxation experiments, the initial nonlinear optical coefficient of all samples d_{33} ($t = 0$) was carefully controlled to be 20 ± 5 pm/V, except for **R**₁ (11 pm/V).

The Kohlrausch–Williams–Watts (KWW) stretched-exponential function is often used to characterize the orientational relaxation of NLO-phores in polymers^{1,3,14,15}

$$d_{33}(t) = d_{33}(0)e^{-(t/\tau)^\beta} \quad (3)$$

where τ is the characteristic relaxation time that is required for the NLO susceptibility $d(t)$ to decay to 1/e of its initial value $d(0)$. The function represents in its original sense a continuous distribution of single expo-

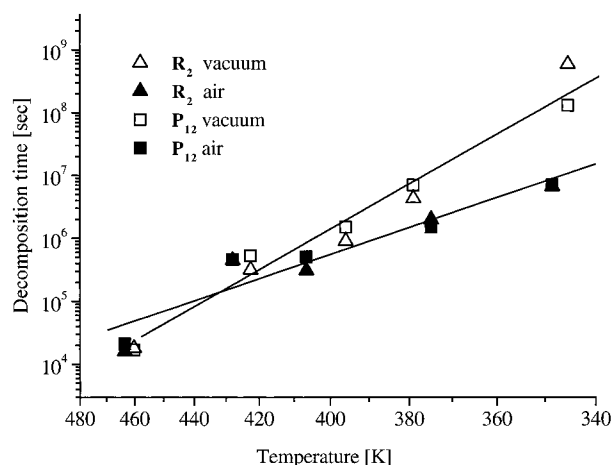


Figure 4. Thermal decomposition times δ of polymers **P**₁₂ and **R**₂ determined in air and vacuum as a function of temperature.

Table 2. Nonlinear Optical Properties of the Main-Chain NLO Polymers

polymer	T_g (°C)	optimum poling temperature (°C)	d_{33} (pm/V) ^a
P ₁₂	125	140	42
R ₁	80	90	11
R ₂	111	120	30
R ₃	131	145	29
BK ₁	80 and 160	125	24

^a Experimental error: $\pm 10\%$.

nential decays where $0 < \beta \leq 1$ is a measure of the width of the distribution and the extent of deviation from single-exponential behavior. We emphasize that in the present study the decay of the nonlinear optical susceptibilities cannot be attributed to a single mechanism because there is evidence for some chemical degradation in addition to the orientational relaxation (see above). However, the KWW function was found suitable to

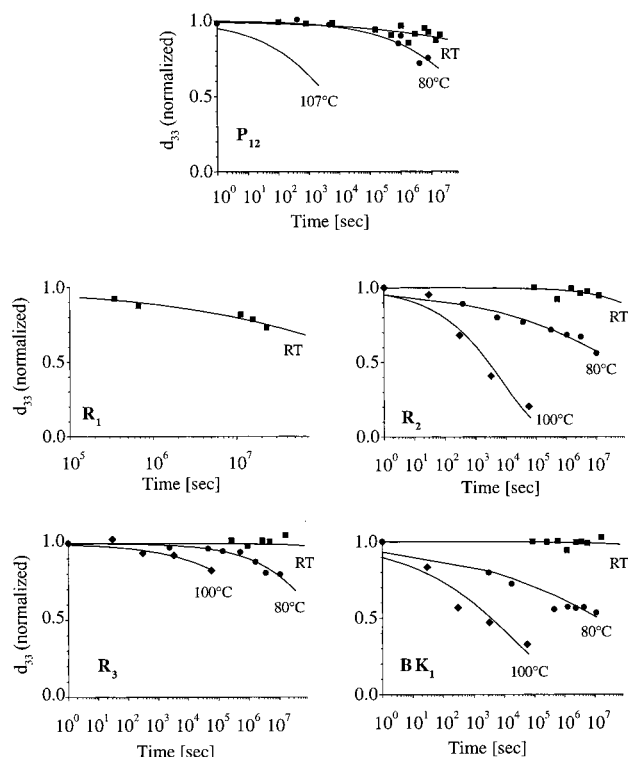


Figure 5. Decay of the normalized nonlinear optical susceptibility of thin films of polymers **P₁₂**, **R₁**, **R₂**, **R₃**, and **BK₁** as a function of time and temperature. Symbols refer to measured data, while the solid lines correspond to stretched-exponential fits.

Table 3. Results of the Relaxation Experiments at Different Temperatures

polymer	β (RT)	τ (RT) (s) ^a	β (80 °C)	τ (80 °C) (s)	β (100 °C)	τ (100 °C) (s)
P₁₂	0.15	2×10^9	0.30	3×10^8 ^b	0.31	1×10^4 ^c
R₁	0.28	3×10^9	not det.	not det.	not det.	not det.
R₂	0.40	2×10^{10}	0.15	5×10^8	0.34	8×10^3
R₃	0.33	2×10^{13}	0.35	6×10^8	0.27	3×10^7
BK₁	0.33	1×10^{13}	0.14	2×10^8	0.23	2×10^4

^a Storage under air. ^b Value for storage under vacuum. Relaxation time for storage under air: 1.66×10^6 s ($\beta = 0.265$) (Weder et al.⁵). ^c Storage under air at 107 °C, data from Weder et al.⁵

describe the decay of the nonlinear optical susceptibilities, especially in the longer time portion of the decay, and the stretched-exponential functions have been fitted to the data according to eq 3. The results are summarized in Table 3.

Before interpreting the relaxation data, one has to compare them with the results from thermal-stability experiments. At 25 °C both processes, thermal degradation and orientational relaxation, are very slow, resulting in a barely detectable decay of the NLO susceptibility, and therefore no statement can be made about which process is the limiting factor. At 80 °C, the relative importance of thermal degradation and decay of the NLO susceptibility are clearly distinguishable; we show data for polymer **R₂** in Figure 6.

Here, the orientational relaxation is the dominant factor under vacuum and *within the investigated time frame*, and thermal decomposition of the NLO-phore can be neglected. However, due to the strongly different nonlinear behavior of the two competing processes, thermal degradation clearly becomes the ascendant process after an aging time of about 36 days under air,

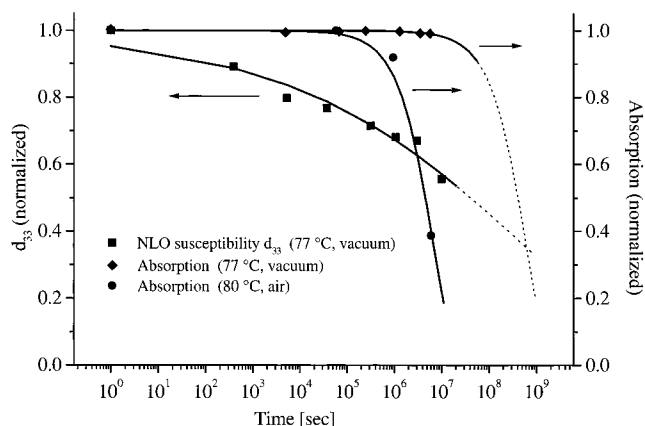


Figure 6. Comparison between thermal degradation of the NLO-phore (as expressed by the decay of the normalized absorption of the NLO-phore's CT band at 474 nm) and the decay of d_{33} (normalized), shown for polymer **R₂** at 80 °C.

as can be seen from the corresponding data. Even when storing the polymeric films in a vacuum, thermal degradation should become the time-limiting step after some years, as the extrapolations (dotted lines) show in Figure 6. Hence, the decrease of the nonlinear optical susceptibilities reported here is mainly due to orientational relaxation within the time frame in which experiments could be made. However, extrapolations to longer aging times would clearly overestimate the stability, because of the increasing importance of thermal decomposition in this time regime.

The determined relaxation times τ range from a few hours (at elevated temperatures) to values of the order of 10^6 years (at 25 °C). While the time interval of 9 months, in which relaxation experiments were undertaken, allows for a reliable estimation of relaxation times in a time regime of a few years, further extrapolations are highly unreliable, because of the reasons discussed above.

As expected, the relaxation times were found to depend on the glass transition temperature of the polymers and the aging temperature; thus the slowest relaxation was observed for polymer **R₃** having the highest T_g of the polymers under investigation. To compare the orientation-relaxation behavior of polymers with different glass transition temperatures T_g , several relations between T_g , the aging temperature, and the relaxation time have been proposed that are related to the Williams-Landel-Ferry (WLF) or the Vogel-Tamann-Fulcher relations.¹⁴⁻¹⁹ Here we employ the scaling relation proposed in refs 14 and 15:

$$\tau(T) = A' \exp\left(\frac{T_g - T}{T}\right) \quad (4)$$

where A' is a constant. The results of the relaxation experiments of the main-chain NLO polymers are plotted in Figure 7 using this scaling relation. For purposes of comparison, the results of similar experiments presented in refs 16 and 17 on guest-host systems (Lophine dye doped in a polyimide matrix, $T_g = 170$ and 190 °C) and of some of us^{14,15} on side-chain polymers (Disperse red 1 attached to a polyimide main chain, $T_g = 130$ and 172 °C) are also included.

As can be seen from Figure 7, the DDANS-based NLO polymers show a significantly enhanced orientational stability when compared to side-chain polymers or guest-host systems, in a temperature regime where

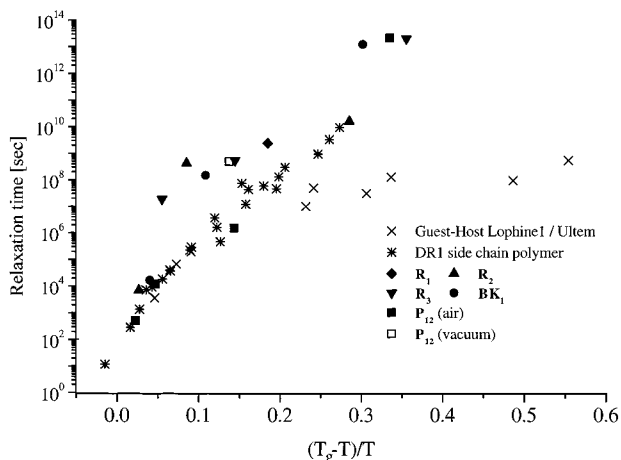


Figure 7. Scaling of relaxation times with $(T_g - T)/T$. DR1: Disperse red 1 attached to polyimide chain.^{14,15} Lophine 1/Ultem: Lophine dye admixed to polyimide matrix.^{16,17}

$(T_g - T)/T > 0.06$. At temperatures close to the glass transition, similar relaxation times are observed for all polymer systems compared.

For the purpose of comparison, we have also included the result of polymeric films of polymer **P**₁₂ stored at 80 °C *under air*, showing a much faster decay of d_{33} due to significant thermal decomposition under these conditions, as shown in Figure 6.

The nature of the relaxation is essentially based on the kind of molecular motion involved in the process. At temperatures close to the glass transition, the motion of the NLO-phores is determined by the mobility of the polymeric matrix and therefore the relaxation times for guest–host, side-chain, and main-chain systems are similar and well described by the WLF relation. WLF is a free volume theory that can only be applied for motions involving a significant part of the polymer chain and, hence, in a temperature regime above or around T_g . At temperatures much below the glass transition, a significant deviation from the WLF behavior is observed because at these temperatures the relaxation is also related to local motions of the NLO-phores (Arrhenius behavior).²⁰ In the case of guest–host systems, the degree of freedom of the NLO-phores is rather high; therefore comparably low relaxation times are observed. For side-chain polymers, motion is restricted because the NLO-phores are covalently bound to the polymeric chain. For main-chain polymers, even higher relaxation times at temperatures below T_g result from the strongly restricting arrangement of the NLO-phores in the polymeric skeleton. Furthermore, decreasing temperatures limit cooperative motion of the polymer chain to such an extent that local motion of the NLO-phore becomes the most important relaxation process and the differences in covalent restrictions between the different classes of structures compared here is strongly evident.

Apparently the hydrogen bond concentration has only little influence on the relaxational stability, as can be deduced when comparing polymers with different contents of amide and ester components. This observation is an indication that the way to link NLO-phores to the polymer backbone is the most critical point for achieving high orientational stability at temperatures below T_g .

Surprisingly, the orientational stability of block copolymer **BK**₁ is comparable to the one of the corresponding random copolymer. Block copolymer **BK**₁

exhibits two T_g 's, as measured by DSC; the T_g of the block of NLO-phores is 160 °C. However, relaxation times at different temperatures of **BK**₁ are comparable to those of **R**₂, and poling conditions were very similar to **R**₂ as well. **BK**₁ is a block copolymer, referring to DSC and matrix-assisted laser desorption ionization mass spectrometry investigations,¹⁰ but with respect to *poling and relaxation processes*, this polymer behaves like a *random copolymer*, possibly because of the low block length of this polymer.

III. Conclusions

The objective of this project was to develop highly stable, poled polymers for NLO and photorefractive applications. Different polymers with NLO-phores incorporated in the polymer main chain were examined.

Thermal aging experiments were performed by monitoring the absorption of the NLO-phore's CT-band as a function of time and temperature. These experiments revealed an Arrhenius decomposition behavior, assuming first-order kinetics. It was demonstrated that thermal decomposition could be significantly reduced by storing the samples in a vacuum instead of air. Although no attempts were made in the present study regarding the decomposition mechanism, this finding is not only important for future studies on the orientational relaxation in NLO polymers but also has technological implications for packaging of EO devices and the stabilization of the active EO materials against chemical degradation.

We have shown that within the time frame of our investigations, orientational relaxation is the dominant process for the decay of nonlinear optical susceptibility. However, due to the strongly nonlinear behavior of the two competing processes, orientational relaxation and thermal degradation, the latter seems to become the ascendant process in a later time regime of the aging process.

The orientational relaxation of the NLO-phores was investigated at different temperatures below the glass transition by the decay of the nonlinear optical susceptibility of corona-poled thin films. The time dependence of the decay was found to be well represented by a KWW stretched-exponential function.

Using the scaling relation $(T_g - T)/T$, a significant difference in relaxation times was observed between the main-chain NLO polymers described here, side-chain NLO systems, as well as guest–host systems described before. It is strongly believed that the most important process for orientational relaxation of the NLO-phores at low temperatures is local motion observable by a deviation from WLF behavior (observed at higher temperatures). Therefore, rigid attachment of the NLO-phores in the polymer backbone is an effective method of reducing this relaxation, more effective than possible for side chain or guest–host systems.

The thermal decomposition process was found to be a limiting factor for the long-term behavior of the nonlinear optical susceptibility of the polymers investigated. The NLO-phore used in our polymers, being based on DANS, is very similar to many commonly employed NLO-phores; hence we suggest that the role of thermal stability of NLO-phores receives special attention. For long-term applications, suitable thermal stabilizers might be used, as is common for commercial technical plastics.

IV. Experimental Section

Materials. Synthesis and characterization of the polymers used in this work are described elsewhere.^{2,10}

Film Preparation. The polymers were dissolved in dry NMP at concentrations of 5% w/w polymer. The solutions were filtered through a 0.45 μm Teflon filter and were spin-cast under heating onto indium–tin-oxide coated glass slides (20 nm, fully oxidized, Balzers Baltracon 217). The samples were dried at 80 °C in a vacuum for at least 12 h. The thickness of the polymer films ranged from 0.4 to 0.8 μm .

Corona Poling. The samples were corona poled with a dc electric field using a tungsten corona needle and a custom-made hotstage as the ground electrode. The applied corona voltage was up to +15 kV at a gap distance of approximately 3 cm. The films were heated under applied field to (5–15) °C above T_g , held at this temperature for about 30 min, and then cooled to 40–60 °C at an average rate of (1.5–3) °C/min.

Aging Experiments. The samples used for long-term aging experiments were always kept in the dark. Samples were stored at room temperature for at least 4 h in the absence of electric fields, to ensure that any residual surface charges from the poling process that might stabilize the noncentrosymmetric orientation had been dissipated.³ Subsequently, the samples were placed on a heavy metal-plate in small, preheated vacuum ovens; the samples reached the desired storing temperature in typically less than 3 min. At elevated temperatures, samples were stored under a dynamic vacuum of 30 mbar. The temperature accuracy was estimated to be 3 °C. Storage at 25 °C was performed under air and normal pressure. Samples were in intervals removed from the oven, rapidly cooled to room temperature, kept at this temperature for about 6 h to perform the susceptibility and absorption measurements, and subsequently returned to the oven. Since the corona poling process applied here was found to result in some inhomogeneity of the NLO-phore's orientation throughout a sample, one spot was marked for each sample, on which all experiments were performed. Susceptibility and absorption experiments were carried out on typically three independent but in most cases simultaneously stored samples, and the obtained data (which revealed a reproducibility of these experiments with an error of less than 10% from one sample to another) were averaged.

Linear and Nonlinear Optical Measurements. All optical experiments were performed as described before.^{2,14} Separate samples were used for relaxation and thermal stability experiments.

Nomenclature

P₁₂: poly{imino-2-[2-(4-(dimethylamino)phenyl)vinyl]-5-nitro-1,4-phenyleneiminocarbonyltetramethylenecarbonyl}-*ran*-{imino-3-[2-(4-(dimethylamino)phenyl)vinyl]-6-nitro-1,4-phenyleneiminocarbonyltetramethylenecarbonyl}

R₁, R₂, R₃: Poly{imino-2-[2-(4-(dimethylamino)phenyl)vinyl]-5-nitro-1,4-phenyleneiminocarbonyltetramethylenecarbonyl}-*ran*-{imino-3-[2-(4-(dimethylamino)phenyl)vinyl]-6-nitro-1,4-phenyleneiminocarbonyltetramethylenecarbonyl}-*oxyethylene*[4-(diphenylhydrazonomethyl)phenyl]imino]ethylenoxycarbonyltetramethylenecarbonyl}

BK₁: poly{oligo-[imino-2-[2-(4-(dimethylamino)phenyl)vinyl]-5-nitro-1,4-phenyleneiminocarbonyltetramethylenecarbonyl]-*ran*-{imino-3-[2-(4-(dimethylamino)phenyl)vinyl]-6-nitro-1,4-phenyleneiminocarbonyltetramethylenecarbonyl}-*block-oligo*-{oxyethylene[4-(diphenyl-

hydrazonomethyl)phenyl]imino]ethylenoxycarbonyltetramethylenecarbonyl}

Acknowledgment. Financial support by the Schweizerischer Nationalfonds zur Förderung der wissenschaftlichen Forschung (NF Sektion II) is gratefully acknowledged.

References and Notes

- (1) See for example: *Nonlinear Optical and Electroactive Polymers*; Prasad, P. N., Ulrich, D. R., Eds.; Plenum Press: New York, 1988. Lytel, R.; Lipscomb, G. F.; Kenney, J. T.; Binkley, E. S. In *Polymers for Lightwave and Integrated Optics*; Hornack, L. A., Ed.; Marcel Dekker: New York, 1992. Burland, D. M.; Miller, R. D.; Walsh, C. A. *Chem. Rev.* **1994**, *94*, 31. *Photorefractive Materials and their Applications*; Günter, P., Huignard, J. P., Eds.; Springer: Berlin, 1988. Moerner, W. E.; Silence, S. M. *Chem. Rev.* **1994**, *94*, 127. Bosshard, Ch.; Sutter, K.; Prêtre, P.; Hülliger, J.; Flörshemer, M.; Kaatz, P.; Günter, P. *Organic Nonlinear Optical Materials*; Gordon and Breach Publishers: Basel, 1995.
- (2) Weder, Ch.; Neuenschwander, P.; Suter, U. W.; Prêtre, P.; Kaatz, P.; Günter, P. *Macromolecules* **1994**, *27*, 2181.
- (3) Weder, Ch.; Neuenschwander, P.; Suter, U. W.; Prêtre, P.; Kaatz, P.; Günter, P. *Macromolecules* **1995**, *28*, 2377.
- (4) Weder, Ch.; Glomm, B. H.; Neuenschwander, P.; Suter, U. W. *Macromol. Chem. Phys.* **1995**, *196*, 1113.
- (5) Weder, Ch.; Neuenschwander, P.; Suter, U. W.; Prêtre, P.; Kaatz, P.; Günter, P. *Nonlinear Opt.* **1996**, *15*, 395.
- (6) Lang, F. R.; Franzreb, K.; Pitton, Y.; Xanthopoulos, N.; Landolt, D.; Mathieu, H. J.; Döbler, M.; Weder, Ch.; Neuenschwander, P.; Suter, U. W. *Proceedings of the 6th European Conference on Application of Surface and Interface Analysis*, ECASIA 1995; Montreux, Switzerland.
- (7) Ahumada, O.; Weder, Ch.; Neuenschwander, P.; Suter, U. W.; Herminghaus, S. *Macromolecules* **1997**, *30*, 3256.
- (8) Weder, Ch.; Glomm, B. H.; Neuenschwander, P.; Suter, U. W.; Prêtre, P.; Kaatz, P.; Günter, P. In *Poled Polymers and Their Applications to SHG and EO Devices*; Miyata, S., Sasabe, H., Eds.; Gordon and Breach Publishers: Basel, 1997.
- (9) Döbler, M.; Weder, Ch.; Neuenschwander, P.; Suter, U. W.; Follonier, S.; Bosshard, C.; Günter, P. *Chimia* **1996**, *50*, 383.
- (10) Döbler, M.; Weder, Ch.; Neuenschwander, P.; Suter, U. W.; Follonier, S.; Bosshard, C.; Günter, P. *Macromolecules* **1998**, *31*, 6124.
- (11) Moylan, C. R.; Swanson, S. A.; Walsh, C. A.; Thackara, J. I.; Twieg, R. J.; Miller, R. D.; Lee, V. Y. *Proc. SPIE* **1993**, *2025*, 192.
- (12) Twieg, R. J.; Betterton, K. M.; Burland, D. M.; Lee, V. Y.; Miller, R. D.; Moylan, C. R.; Volksen, W.; Walsh, C. A. *Proc. SPIE* **1993**, *2025*, 94.
- (13) Twieg, R. J.; Burland, D. M.; Hedick, J. L.; Lee, V. Y.; Miller, R. D.; Moylan, C. R.; Volksen, W.; Walsh, C. A. *Mater. Res. Soc. Symp. Proc.* **1994**, *328*, 421.
- (14) Prêtre, P.; Kaatz, P.; Bohren, A.; Günter, P.; Zysset, B.; Ahlheim, M.; Stähelin, M.; Lehr, F. *Macromolecules* **1994**, *27*, 5476.
- (15) Kaatz, P.; Prêtre, P.; Meier, U.; Stalder, U.; Bosshard, C.; Günter, P. *Macromolecules* **1996**, *29*, 1666.
- (16) Walsh, C. A.; Burland, D. M.; Lee, V. Y.; Miller, R. D.; Smith, B. Y.; Twieg, R. J.; Volksen, W. *Macromolecules* **1993**, *26*, 3720.
- (17) Stähelin, M.; Walsh, C. A.; Burland, D. M.; Miller, R. D.; Twieg, R. J.; Volksen, W. *J. Appl. Phys.* **1993**, *73*, 8471.
- (18) Goodson, T., III; Wang, C. H. *Macromolecules* **1993**, *26*, 1837.
- (19) Chen, J. I.; Marturunkakul, S.; Li, L.; Jeng, R. J.; Kumar, J.; Tripathy, S. K. *Macromolecules* **1993**, *26*, 7379.
- (20) Dhinojwala, A.; Hooker, J. C.; Torkelson, J. M. *Polymers for Second Order Nonlinear Optics*; American Chemical Society: Washington, DC, 1995.

MA981054K